

Modification of the Phased-Tracking Method for Reduction of Artifacts in Estimated Artery Wall Deformation

Hideyuki Hasegawa, *Member, IEEE*, and Hiroshi Kanai, *Member, IEEE*

Abstract—Noninvasive measurement of mechanical properties, such as elasticity, of the arterial wall, is useful for diagnosis of atherosclerosis. For assessment of mechanical properties, it is necessary to measure the deformation of the arterial wall. In this study, a modification of the previously proposed phased-tracking method was conducted to improve measurement of the small change in thickness (deformation) of the arterial wall due to the heartbeat. In our previous method, a set of two points along an ultrasonic beam was initially assigned, and the change in thickness of the layer between these two points during an entire cardiac cycle was estimated. In motion estimation with ultrasound, the motion of an interface or a scatterer, which generates an echo, can be obtained by estimating the change in time delay of the echo. For example, in the case of a carotid artery of a healthy subject, there are only two dominant echoes from the lumen-intima and media-adventitia interfaces. Thus, only the displacements of the lumen-intima and media-adventitia interfaces can be estimated, which means that ultrasound can estimate only the change in distance (thickness) between these two interfaces. However, even in this case, our previous method gives different estimates of the change in thickness, depending on the depths (positions in the arterial radial direction) of the two initially assigned points. In this study, modifications of the previous method in terms of the strategy for assignment of layers and the required thickness of an assigned layer were made to reduce such an artificial spatial variation in the estimated changes in thickness. Using the proposed method, errors in estimated changes in thickness were reduced from $21.2 \pm 24.1\%$ to $0.19 \pm 0.04\%$ (mean \pm standard deviation) in simulation experiments. As in the case of the simulation experiments, the spatial variation in estimated changes in thickness also was reduced in *in vivo* experiments in a carotid artery of a healthy subject and *in vitro* experiments using two excised, diseased arteries.

I. INTRODUCTION

NONINVASIVE measurement of mechanical properties of the arterial wall, such as elasticity, is useful for diagnosing atherosclerosis because there are significant differences between the elastic moduli of normal arterial walls and those affected by atherosclerosis [1], [2].

For assessment of mechanical properties, various methods have been proposed to measure the displacement of the arterial wall. Elasticity based on estimation of the pulse

wave velocity (PWV) [3]–[6] and the homogeneity of distensibility [7], which is evaluated by the change in diameter obtained from displacements of near and far walls, can be noninvasively evaluated by measuring displacements at multiple points in the axial direction of the artery. Of course, measurement of the change in diameter at one point is widely used for assessment of mechanical properties of the arterial wall [8]–[10]. In such case, however, the arterial wall must be assumed to be an isotropic, cylindrical shell with a uniform wall thickness.

In addition to the displacement distribution in the axial direction of the artery, the distribution in the radial direction of the arterial wall has been measured with intravascular ultrasonography (IVUS) [11], [12]. The elasticity distribution of coronary atherosclerotic plaque has been obtained [12] based on the measurement of the radial strain [11]. Furthermore, model-based methods have been proposed for improving the strain estimation [13]. In those studies, such a measured elasticity distribution was compared with the pathological image and suggested the potential for tissue characterization of atherosclerotic plaque by measurement of its elasticity.

As a transcutaneous approach, the displacement and strain around carotid atherosclerotic plaque have been measured using tissue Doppler imaging [14]. The inhomogeneity of displacements measured upstream and downstream of atherosclerotic plaque suggested that motion of the arterial wall has potential for use in the evaluation of plaque vulnerability. Furthermore, in recent years, some research studies on noninvasive vascular elastography have been conducted [15], [16].

We previously developed a method, namely, the phased-tracking method, for measuring small vibrations on the heart or arterial wall with transcutaneous ultrasound [17], [18]. For some years now, we have been measuring the displacement and change in thickness of the arterial wall caused by the heartbeat using this method [19]–[21]. Elasticity images of the human carotid artery have been obtained by the measured displacement distribution, and the potential for transcutaneous tissue characterization has been shown by classifying the elasticity images using the elasticity reference data obtained by *in vitro* experiments [22]–[24].

Although the noninvasive methods for measuring the intima-media thickness [25] and lumen diameter [26] based on the automated image segmentation are useful for diagnosis of the morphology of the arterial wall and atheroscle-

Manuscript received October 22, 2005; accepted May 28, 2006.

The authors are with the Department of Electronic Engineering, Graduate School of Engineering, Tohoku University, Sendai 980-8579, Japan (e-mail: hasegawa@us.ecei.tohoku.ac.jp).

Digital Object Identifier 10.1109/TUFFC.2006.145

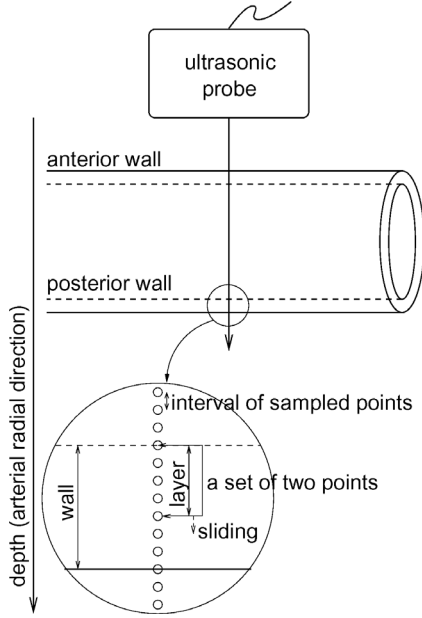


Fig. 1. Schematic of measurement.

rotic plaque, the measurements of mechanical properties—including our method—also are important because myocardial infarction and stroke are mainly caused by the rupture of atherosclerotic plaque [27], [28].

In the phased-tracking method, the small deformation of the arterial wall can be detected based on precise estimation of the velocity of the arterial wall. The velocity is estimated by the phase shift of echoes that corresponds to the change in the time delay for two-way propagation of ultrasound between an ultrasonic probe and the arterial wall. The phase shift can be estimated at each frequency within the frequency bandwidth of an echo. However, we recently revealed that the estimated velocity is biased unless the phase shift is estimated at the center frequency of an echo [29]. Although this error is not so large during a frame interval, the estimated velocity must be integrated with respect to time for tracking the position of the arterial wall. Therefore, this error becomes significant due to accumulation resulting from temporal integration.

In this study, a source of error in estimation of the deformation of the arterial wall was investigated. In our previous phased-tracking method [20], [21], [23], a set of two points was assigned along an ultrasonic beam as shown in Fig. 1, and the change in thickness of the layer between these two points was estimated. Furthermore, by sliding the position of the layer along an ultrasonic beam by intervals of the sampled points, the spatial distribution of changes in thickness along the ultrasonic beam was obtained.

In such a motion estimation with ultrasound, the motion of an interface or a scatterer, which generates an echo, can be obtained by estimating the change in time delay of the echo. For example, in the case of a carotid artery of a healthy subject, there are only two dominant echoes from the lumen-intima and media-adventitia in-

terfaces [30]. Thus, only the displacements of the lumen-intima and media-adventitia interfaces can be estimated, which means that ultrasound can estimate only the change in distance (thickness) between these two interfaces. However, even in such a case, the previous phased-tracking method gives different estimates of the change in thickness, depending on the depths (positions in the arterial radial direction) of the two initially assigned points. In this study, modifications of the previous method in terms of the strategy for assignment of layers and the required thickness of a layer were made to reduce such an artificial spatial variation in the estimated changes in thickness.

In the estimation of the change in thickness using the correlation estimator, the thickness of an assigned layer is larger than the interval of sampled points, and the layer is slid by the interval of sampled points. Therefore, several layers with respective correlation estimators overlap at each depth. In this study, correlation estimators of layers, which overlap at a certain depth, were compounded to obtain the change in thickness at that depth. Although the angle of the ultrasonic beam was not changed in this study, the concept of spatial compounding already has been applied to magnitudes of echoes, which are obtained by scanning each point in the region of interest with ultrasonic beams having different beam angles, to improve B-mode images [31].

II. METHODS

A. Previously Proposed Phased-Tracking Method for Imaging Radial Deformation of Arterial Wall

Radio frequency (RF) pulses with a center frequency of f_0 are transmitted with a time interval T from an ultrasonic transducer, and the echo reflected by an interface or a scatterer is received by the same transducer as shown in Fig. 2. The propagation delay, $\tau_1(n)$, between the transducer and the reflector (interface or scatterer) at n -th transmission (frame) depends on the sound speed, c_0 , and the distance $d_1(n)$ between the transducer and the reflector:

$$\tau_1(n) = \frac{2d_1(n)}{c_0} \quad (1)$$

$(n = 1, 2, \dots, N; N: \text{number of frames}).$

Phase $\theta_1(n)$ of a received echo is expressed by $\theta_1(n) = 2\pi f_0 \tau_1(n)$ at the center frequency, f_0 . Therefore, distances $d_1(n)$ and $d_1(n+1)$ between the ultrasonic transducer and the reflector in n -th and $(n+1)$ -th frames are given by:

$$d_1(n) = \frac{c_0 \tau_1(n)}{2} = \frac{c_0}{4\pi f_0} \cdot \theta_1(n), \quad (2)$$

$$d_1(n+1) = \frac{c_0 \tau_1(n+1)}{2} = \frac{c_0}{4\pi f_0} \cdot \theta_1(n+1). \quad (3)$$

The average velocity of the reflector during a frame interval, T , is defined by $v_1(n) = \{d_1(n+1) - d_1(n)\}/T$.

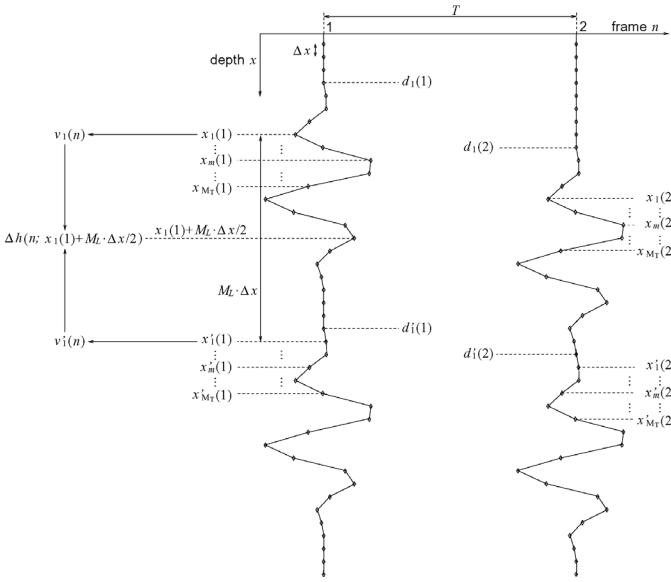


Fig. 2. Estimation of the change in thickness of the arterial wall by the previously proposed phased-tracking method. (M_T : total number of assigned combinations, M_L : number of sampled points between two points of an assigned combination, T : frame interval, Δx : spacing of sampled points, $d_1(n)$ and $d'_1(n)$: depths of the lumen-intima and media-adventitia interfaces in n -th frame, $x_m(n)$ and $x'_m(n)$: m -th combination of two points in n -th frame, $v_m(n)$ and $v'_m(n)$: velocities at $x_m(n)$ and $x'_m(n)$, respectively, $\Delta h(n, x)$: change in thickness at depth x in n -th frame).

Thus, $v_1(n)$ can be estimated from phase shift $\Delta\theta_1(n) = \theta_1(n+1) - \theta_1(n)$ of echoes as follows:

$$\begin{aligned} v_1(n) &= \frac{d_1(n+1) - d_1(n)}{T} \\ &= \frac{c_0(\tau_1(n+1) - \tau_1(n))}{2T} \\ &= \frac{c_0}{4\pi f_0 T} \cdot \Delta\theta_1(n). \end{aligned} \quad (4)$$

To obtain phase $\theta_1(n)$ of an RF echo, the quadrature demodulation at the center frequency, f_0 , is applied to sampled RF echoes, and the sampled complex demodulated signal, $z(n; x)$, is obtained along an ultrasonic beam (x -axis).

As shown in Fig. 2, by referring to an M-mode image, initial depth $x_1(1) \approx d_1(1)$ is manually assigned as the position of the reflector at the first frame. Initial depth $x_1(1)$ usually does not exactly correspond to $d_1(1)$ due to the manual assignment. However, phase shift $\Delta\theta_1(n)$ can be estimated at $x_1(n)$ because the ultrasonic pulse used has a finite-pulse duration as shown in Fig. 2. When $x_1(1)$ is within the duration of the echo from $d_1(1)$, phase $\angle z(n; x_1(n))$ of the complex demodulated signal, $z(n; x_1(n))$, at depth $x_1(n)$ corresponds to $\theta_1(n)$:

$$\theta_1(n) = \angle z(n; x_1(n)). \quad (5)$$

Thus, phase shift $\Delta\theta_1(n) = \theta_1(n+1) - \theta_1(n)$ between two consecutive frames is estimated by the well-known autocorrelation function calculated as follows [17]:

$$\begin{aligned} e^{j\Delta\theta_1(n)} &= \\ &= \frac{\sum_{k=-K/2}^{K/2} z^*(n; x_1(n) + k \cdot \Delta x) \cdot z(n+1; x_1(n) + k \cdot \Delta x)}{\left| \sum_{k=-K/2}^{K/2} z^*(n; x_1(n) + k \cdot \Delta x) \cdot z(n+1; x_1(n) + k \cdot \Delta x) \right|} \\ &= \widehat{r}_1(n), \end{aligned} \quad (6)$$

where Δx is the interval of the sampled demodulated signal in the depth direction; $*$ and $\widehat{}$ represent the complex conjugate and the estimate. In this study, the number of sampled points, K , used for calculation of the correlation function is determined by the width at -20 dB of the maximum magnitude of the quadrature demodulated signal of the ultrasonic pulse. From the estimated correlation function $\widehat{r}_1(n)$ obtained by (6), average velocity $v_1(n)$ during the frame interval, T , is obtained as follows:

$$\widehat{v}_1(n) = \frac{c_0}{4\pi f_0 T} \cdot \widehat{\Delta\theta}_1(n) = \frac{c_0}{4\pi f_0 T} \cdot \angle \widehat{r}_1(n), \quad (7)$$

where $\angle r_1(n)$ represents the phase of the complex correlation function $r_1(n)$.

In the estimation of the phase shift by (6), instantaneous position $x_1(n)$ of the assigned point is tracked by accumulation of displacement $\widehat{v}_1(n) \cdot T$ during a frame interval, T , as follows:

$$\widehat{x}_1(n+1) = \widehat{x}_1(n) + \widehat{v}_1(n) \cdot T. \quad (8)$$

When there are two reflectors (interface or scatterer) at different depths of $d_1(n)$ and $d'_1(n)$, the change in thickness of the layer between these two reflectors is obtained as follows: By referring to an M-mode image, initial position $x_1(1) \approx d_1(1)$ is manually assigned at the first frame as the position of the lumen-intima interface. Then, as shown in Fig. 2, another point, $x'_1(1) = x_1(1) + M_L \cdot \Delta x$, is automatically assigned at certain distance, $M_L \cdot \Delta x$, from $x_1(1)$ along the same ultrasonic beam. When $x'_1(1)$ corresponds to the position of the echo from another reflector at $d'_1(1)$, the motion of the reflector can be estimated.

Then, velocities $v_1(n)$ and $v'_1(n)$ of these assigned points are obtained by tracking their instantaneous positions $x_1(n)$ and $x'_1(n)$ as described above. In the previously proposed phased-tracking method, from estimated velocities $\widehat{v}_1(n)$ and $\widehat{v}'_1(n)$, change in thickness $\Delta h(n; x)$ of the layer between the two assigned points $x_1(1)$ and $x'_1(1) = x_1(1) + M_L \cdot \Delta x$ is obtained as the deformation at a depth of $x_1(1) + M_L \cdot \Delta x/2$ as follows [23]:

$$\begin{aligned} \widehat{\Delta h}(n+1; x_1(1) + M_L \cdot \Delta x/2) &= \\ &= \widehat{\Delta h}(n; x_1(1) + M_L \cdot \Delta x/2) + \left\{ \widehat{v}'_1(n) - \widehat{v}_1(n) \right\} \cdot T, \\ \widehat{\Delta h}(1; x_1(1) + M_L \cdot \Delta x/2) &= 0. \end{aligned} \quad (9)$$

By sliding the combination of two points along the ultrasonic beam while keeping the distance between two

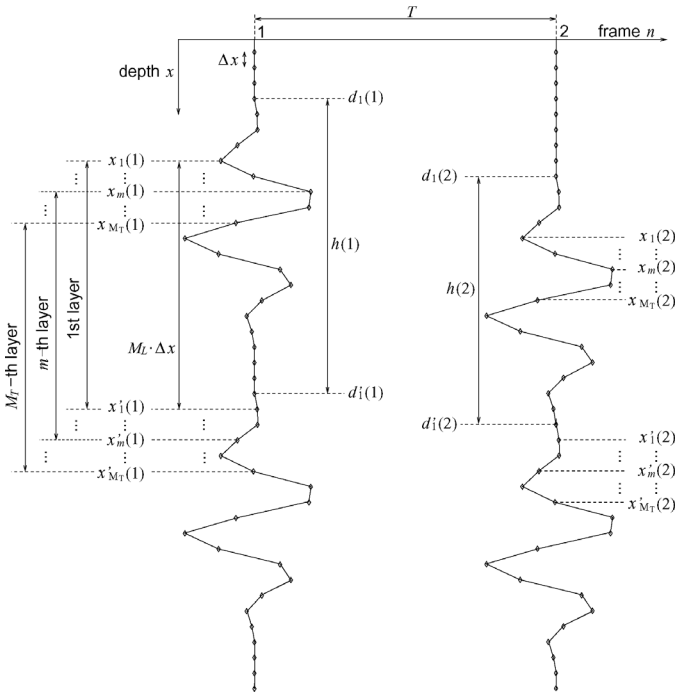


Fig. 3. Modified method for estimation of the change in thickness of the arterial wall (M_T : total number of assigned combinations, M_L : number of sampled points between two points of an assigned combination, T : frame interval, Δx : spacing of sampled points, $d_1(n)$ and $d'_1(n)$: depths of the lumen-intima and media-adventitia interfaces in n -th frame, $x_m(n)$ and $x'_m(n)$: m -th combination of two points in n -th frame, $h(n)$: distance between the lumen-intima and media-adventitia interfaces in n -th frame).

points constant ($= M_L \cdot \Delta x$), the change in thickness $\Delta h(n; x_m(1) + M_L \cdot \Delta x/2)$ at each depth is obtained as follows:

$$\begin{aligned} \widehat{\Delta h}(n+1; x_m(1) + M_L \cdot \Delta x/2) &= \widehat{\Delta h}(n; x_m(1) \\ &+ M_L \cdot \Delta x/2) + \left\{ \widehat{v}'_m(n) - \widehat{v}_m(n) \right\} \cdot T, \\ \widehat{\Delta h}(1; x_m(1) + M_L \cdot \Delta x/2) &= 0, \end{aligned} \quad (10)$$

$$x_m(1) = x_1(1) + m \cdot \Delta x, \quad (m = 0, 1, 2, \dots, M_T), \quad (11)$$

where M_T is the manually determined number of times that sliding occurs.

B. Modification of the Phased-Tracking Method and Correlation Estimator Compounding

In this section, the previously proposed phased-tracking method is modified [21] with correlation estimator compounding.

As in Section II-A, by referring to an M-mode image, initial positions $x_1(1)$ and $x'_1(1)$ of two points are manually assigned at the first frame as shown in Fig. 3 ($x'_1(1) - x_1(1) = M_L \cdot \Delta x$). Then, instantaneous positions $x_1(n)$ and $x'_1(n)$ of these assigned points at the n -th frame are tracked by the method described in Section II-A.

The change in thickness between two reflectors at $d_1(n)$ and $d'_1(n)$ then is obtained as follows. As shown by (2), phases $\theta_1(n)$ and $\theta'_1(n)$ of echoes from these two reflectors depend on $d_1(n)$ and $d'_1(n)$. Thus, the phase difference $\theta_h(n) = \theta'_1(n) - \theta_1(n)$ depends on the distance $h(n) = d'_1(n) - d_1(n)$ (thickness of the layer) between two reflectors as follows:

$$\begin{aligned} h(n) &= d'_1(n) - d_1(n) \\ &= \frac{c_0}{4\pi f_0} \{ \theta'_1(n) - \theta_1(n) \} \\ &= \frac{c_0}{4\pi f_0} \cdot \theta_h(n). \end{aligned} \quad (12)$$

Thus, as in the case of (4), the rate $v_h(n)$ of the change in thickness of the layer between two reflectors is expressed as follows:

$$\begin{aligned} v_h(n) &= \frac{h(n+1) - h(n)}{T} \\ &= \frac{c_0}{4\pi f_0 T} \{ \theta_h(n+1) - \theta_h(n) \} \\ &= \frac{c_0}{4\pi f_0 T} \cdot \Delta \theta_h(n). \end{aligned} \quad (13)$$

As in the case of (5), when $x_1(1)$ and $x'_1(1)$ assigned as shown in Fig. 3 are within the durations of the echoes from $d_1(1)$ and $d'_1(1)$, phase difference $\theta_h(n)$ can be expressed by phase $\angle \beta(n; x_1(1), x'_1(1))$ of product $\beta(n; x_1(1), x'_1(1))$ of complex demodulated signals, $z(n; x_1(n))^*$ and $z(n; x'_1(n))$, as follows:

$$\theta_h(n) = \theta'_1(n) - \theta_1(n) = \angle \beta(n; x_1(n), x'_1(n)), \quad (14)$$

$$\beta(n; x_1(n), x'_1(n)) = z(n; x'_1(n)) \cdot z^*(n; x_1(n)). \quad (15)$$

In this paper, correlation estimator $r_h(n; x)$ at depth x , whose phase $\angle r_h(n; x)$ corresponds to $\theta_h(n+1) - \theta_h(n) = \Delta \theta_h(n)$, is obtained by simply calculating the correlation around the duration of echo as follows:

$$\begin{aligned} \widehat{r}_h(n; x_1(1) + i \cdot \Delta x) &= \sum_{k=-K/2}^{K/2} \beta(n+1; x_1(n) \\ &+ k \cdot \Delta x, x'_1(n) + k \cdot \Delta x) \cdot \beta^*(n; x_1(n) \\ &+ k \cdot \Delta x, x'_1(n) + k \cdot \Delta x), \\ &(i = 0, 1, 2, \dots, M_L), \end{aligned} \quad (16)$$

where the estimate in the right-hand side of (16) is used for correlation estimators $r_h(n; x)$ at all points between $x_1(1)$ and $x'_1(1)$ in the modified method, whereas the change in thickness between points $x_1(1)$ and $x'_1(1)$ is used only for the point that is midway between these two points, as shown by (9) in the previous method.

As with (10), by sliding the combination of two points along the ultrasonic beam while keeping the distance between the two points constant ($= M_L \cdot \Delta x$), the correlation

estimator, $r_{h,m}(n; x)$, for each combination of two points, $x_m(1)$ and $x'_m(1)$, is obtained as follows:

$$\begin{aligned} \widehat{r_{h,m}}(n; x_m(1) + i \cdot \Delta x) = & \sum_{k=-K/2}^{K/2} \beta(n+1; x_m(n)) \\ & + k \cdot \Delta x, x'_m(n) + k \cdot \Delta x \cdot \beta^*(n; x_m(n)) \\ & + k \cdot \Delta x, x'_m(n) + k \cdot \Delta x, \end{aligned} \quad (17)$$

$$\begin{aligned} x_m(1) = x_1(1) + m \cdot \Delta x, \\ (m = 0, 1, 2, \dots, M_T; i = 0, 1, 2, \dots, M_L), \end{aligned} \quad (18)$$

where M_T is the manually assigned number of times that sliding occurs.

As shown in Fig. 3, M_T assigned layers overlap each other. Therefore, there are multiple estimates of $r_h(n; x)$ at a depth x . The compounded correlation estimator, $\bar{r}_h(n; x)$, at depth x then is obtained by simply averaging overlapping correlation estimators as follows:

$$\bar{r}_h(n; x_m(1)) = \frac{1}{M_O(x_m(1))} \sum_{k=m}^{m+M_O(x_m(1))} \widehat{r_{h,k}}(n; x_m(1)), \quad (19)$$

where $M_O(x)$ is the number of overlapping layers at depth x .

The compounded rate, $\bar{v}_h(n; x)$, of the change in thickness at depth x is obtained based on (13) as follows:

$$\bar{v}_h(n; x_m(1)) = \frac{c_0}{4\pi f_0 T} \cdot \angle \bar{r}_h(n; x_m(1)). \quad (20)$$

The compounded change in thickness, $\Delta \bar{h}(n; x)$, is obtained as follows:

$$\Delta \bar{h}(n+1; x_m(1)) = \Delta \bar{h}(n; x_m(1)) + \bar{v}_h(n; x_m(1)) \times T. \quad (21)$$

The estimation of the velocity or rate of the change in thickness depends on the phase shift of received echoes, and the velocity is larger than the rate of the change in thickness. Therefore, the required frame rate is determined by the velocity of the arterial wall. The maximum velocity of the carotid arterial wall is typically about 10 mm/s. Thus, when the ultrasound center frequency and speed of sound are 7.5 MHz and 1540 m/s, respectively, the required frame rate, FR_{\min} , is determined by substituting $v_1(n) = 10$ mm/s and $\Delta\theta_1(n) = \pi$ into (4) as follows:

$$FR_{\min} = \frac{4\pi \times 7.5 \times 10^6 \times 10 \times 10^{-3}}{1540 \times \pi} = 195 \text{ Hz}. \quad (22)$$

In addition, the deformation estimate by the proposed method depends on the time delay of an echo during two-way propagation between an ultrasonic probe and a reflector along an ultrasonic beam. Therefore, only the beam-axis component of the deformation can be measured by the proposed method.

III. DRAWBACKS OF PREVIOUSLY PROPOSED PHASED-TRACKING METHOD

Fig. 4(a) shows a B-mode image of a carotid artery of a 30-year-old, healthy male. The B-mode image was acquired using a 10 MHz linear-type ultrasonic probe of ultrasonic diagnostic equipment (SSD-6500, Aloka Co., Ltd., Tokyo, Japan). Figs. 4(b) and (c) show RF echoes from the posterior wall along the white arrow in Fig. 4(a). The region shown in Figs. 4(b) and (c) is indicated by a white dashed line in Fig. 4(a). In healthy subjects, there are only two dominant echoes from the lumen-intima and media-adventitia interfaces [30]. In this study, as shown in Figs. 4(b) and (c), the intima-media thickness (IMT) is defined by the region between the rises of echoes from the lumen-intima and media-adventitia interfaces. In this study, these rises were manually assigned by inspecting a B-mode or M-mode image. In motion estimation with ultrasound, we can estimate the motion of a reflector (interface or scatterer) by analyzing its echo. Therefore, in the case of a healthy subject, we can estimate only displacements of the lumen-intima and media-adventitia interfaces. Thus, only the change in thickness between these interfaces, which corresponds to the change in the entire intima-media thickness, can be obtained. As described in [11], the deformation at a point in a cylindrical shell changes in relation to its radial position, and such a change depending on the radial position could be measured in [11] because there were many scatterers generating dominant echoes within the wall of the cylindrical phantom used.

As shown in Fig. 4(b), however, in cases of arteries of healthy subjects, there are only two dominant echoes from two corresponding reflectors (lumen-intima and media-adventitia interfaces). Under such a condition, although multiple points can be assigned as shown in Fig. 2, each assigned point gives the displacement of the lumen-intima or media-adventitia interface. Therefore, only the deformation between two reflectors, which corresponds to the change in thickness of the entire intima-media complex, can be obtained; but the deformation at a point in the wall cannot be measured in such a situation.

However, changes in thickness obtained by the previously proposed phased-tracking method change depending on depth (radial position in the wall), even when there are only two reflectors. The reason for this is considered to be as follows. At the first frame, the lumen-intima and media-adventitia interfaces are manually assigned as shown in Fig. 4(b) by inspecting an M-mode image (or B-mode image). As shown in Fig. 4(b), there usually are discrepancies between the manually assigned interfaces and actual interfaces due to the manual assignment based on an M-mode image. Then, the first combination of the two points $x_1(1)$ and $x'_1(1)$ is assigned as shown in Fig. 4(b) to obtain the change in thickness at a certain depth, which corresponds to the manually assigned lumen-intima interface. The thickness of a layer, $M_L \cdot \Delta x$, is assigned to be the width at -6 dB of the maximum magnitude of the quadrature demodulated signal of the ultrasonic pulse in

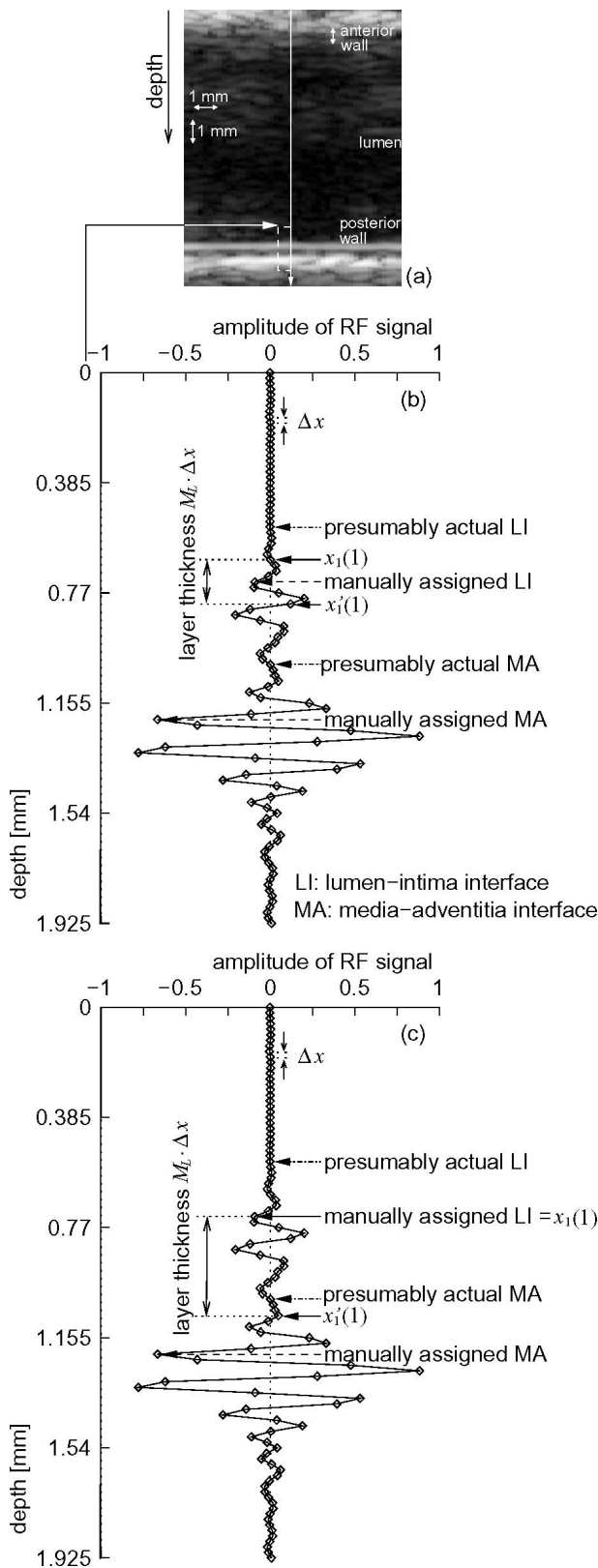


Fig. 4. (a) B-mode image of a carotid artery of a 30-year-old, healthy male. White dashed line in the B-mode image shows the region shown in (b) and (c). (b) Assignment of the first layer (between two points $x_1(1)$ and $x'_1(1)$) in the previous phased-tracking method. LI and MA are acronyms for the lumen-intima and media-adventitia interfaces, respectively. (c) Assignment of $x_1(1)$ and $x'_1(1)$ in the proposed method.

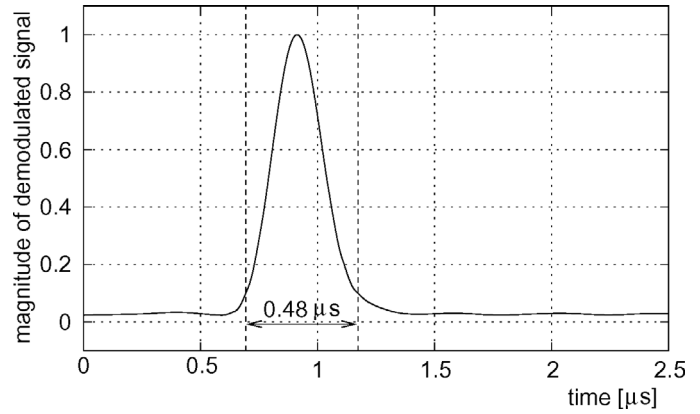


Fig. 5. Magnitude of the quadrature demodulated signal of the ultrasonic pulse used measured with a hydrophone placed in a water tank.

the previous phased-tracking method [23]. In a situation such as that shown in Fig. 4(b), $x_1(1)$ and $x'_1(1)$ are assigned within the same echo from the lumen-intima interface. Therefore, both displacements, estimated at $x_1(1)$ and $x'_1(1)$, correspond to that of the lumen-intima interface (high similarity of these two displacements). Thus, the change in thickness (difference between these two displacements) is hardly detected. This is just an artifact due to the finite duration of the ultrasonic pulse.

In the modified method in this study, $x_1(1)$ and $x'_1(1)$ are assigned as shown in Fig. 4(c). To prevent $x'_1(1)$ from being assigned within the duration of the same echo from the lumen-intima interface, a larger thickness of a layer, $M_L \cdot \Delta x$, is necessary in comparison with the previous method. Therefore, the required thickness of a layer, $M_L \cdot \Delta x$, is investigated in Section IV-C.

In the simulation experiments in this study, the required thickness of a layer, $M_L \cdot \Delta x$, was investigated in relation to the width of the magnitude of the quadrature demodulated signal of the ultrasonic pulse used. Fig. 5 shows the magnitude of the demodulated signal of the ultrasonic pulse used measured with a hydrophone placed in a water tank. The hydrophone was placed at a distance of 20 mm from the surface of a linear-type probe, which corresponds to the electric focal depth. The RF signal received by the hydrophone was acquired at a sampling frequency of 1 GHz with a digital oscilloscope. Quadrature demodulation was applied to the sampled RF signal.

IV. SIMULATION EXPERIMENTS

A. Principle for Simulating RF Echoes from Normal Arterial Walls

An RF echo signal, $rf(n; x)$, in the n -th frame at depth x , which is reflected from the arterial wall of a healthy subject, can be modeled by the sum of echoes, $rf_{LI}(n; x)$ and $rf_{MA}(n; x)$, from the lumen-intima and media-adventitia interfaces, respectively, located at depths $d_{LI}(n)$ and

$d_{MA}(n)$. In such a situation, $rf(n; x)$ is expressed using a sinusoidal wave at the center frequency f_0 and the envelope $env(x)$ as follows:

$$rf(n; x) = rf_{LI}(n; x) + rf_{MA}(n; x), \quad (23)$$

$$rf_{LI}(n; x) = env(x - d_{LI}(n)) \cdot \sin \left\{ \frac{4\pi f_0(x - d_{LI}(n))}{c_0} \right\}, \quad (24)$$

$$rf_{MA}(n; x) = env(x - d_{MA}(n)) \cdot \sin \left\{ \frac{4\pi f_0(x - d_{MA}(n))}{c_0} \right\}, \quad (25)$$

$$env(x) = \begin{cases} 0.5 - 0.5 \cdot \cos \left\{ 2\pi \frac{x}{\Delta X_p} \right\} & (0 \geq x \geq \Delta X_p), \\ 0 & (\Delta X_p < x), \end{cases} \quad (26)$$

where ΔX_p is the pulse duration. In this study, a Hann window was used for the envelope of an ultrasonic pulse, and the center frequency, pulse duration, frame rate, and sampling frequency of simulated echoes were 7.5 MHz, 3 wavelengths, 286 Hz, and 40 MHz, respectively.

Displacements of the posterior carotid artery wall of a healthy, 30-year-old male [same as Fig. 4(a)], which were measured by the phased-tracking method described in Section II-A, were used as displacements of the lumen-intima and media-adventitia interfaces, $\Delta d_{LI}(n) = d_{LI}(n) - d_{LI}(1)$ and $\Delta d_{MA}(n) = d_{MA}(n) - d_{MA}(1)$.

As described in Section III, in the case of a healthy subject, there are only two dominant echoes from the lumen-intima and media-adventitia interfaces, and only the change in the entire intima-media thickness can be estimated by analyzing echoes from these interfaces. Therefore, the change in intima-media thickness, $\Delta h_{IMT}(n) = \Delta d_{MA}(n) - \Delta d_{LI}(n)$, was defined as the true deformation. Errors, e_h , in changes in thickness, $\widehat{\Delta h}(n; x)$ and $\Delta \bar{h}(n; x)$, estimated by the previous and proposed methods were obtained as follows:

$$e_h = \frac{|\Delta h(n_{\max}) - \Delta h_{IMT}(n_{\max})|}{|\Delta h_{IMT}(n_{\max})|} \times 100, \quad (27)$$

where $\Delta h(n)$ is $\widehat{\Delta h}(n; x)$ or $\Delta \bar{h}(n; x)$, and $t_{\max} = n_{\max} \cdot T$ is the time when $\Delta h_{IMT}(n)$ is maximum.

B. Improvement of Deformation Estimates Using the Proposed Method

Fig. 6(a) shows RF echo lines simulating those reflected from the lumen-intima and media-adventitia interfaces during one heart cycle. Fig. 6(b) shows the M-mode image obtained from the simulated RF echo lines shown in Fig. 6(a). In this section, the initial intima-media thickness, $d_{MA}(1) - d_{LI}(1)$, at the first frame in (24) and (25) was set at 0.45 mm, which was obtained from Fig. 4. By referring to the M-mode image shown in Fig. 6(b), the initial positions of the lumen-intima and media-adventitia boundaries were assigned manually at the first frame (time

$t = 0$). With respect to multiple points between the assigned lumen-intima and media-adventitia boundaries, velocities, $v_m(n)$, at each frame were estimated as shown in Fig. 6(c), and the instantaneous position of each point, $x_m(n)$, was tracked using the phased-tracking method. The estimated instantaneous positions of the lumen-intima and media-adventitia boundaries are shown by white lines in Fig. 6. Based on the instantaneous positions of the points assigned at $t = 0$ between the lumen-intima and media-adventitia boundaries, the rate of change in thickness at each depth, $x_m(n)$, was obtained by the previous and proposed methods as shown in Figs. 6(d) and (e), respectively. In Fig. 6(e), the thickness of a layer, $M_L \cdot \Delta x$, was set to be the width at -20 dB of the maximum magnitude of the quadrature demodulated signal shown in Fig. 5. The width at -20 dB was determined to be $0.48 \mu\text{s}$, which corresponds to a distance of $370 \mu\text{m}$ at a sound speed of 1540 m/s . Along the instantaneous positions of each point at respective frames, the rate of change in thickness was integrated with respect to time, and the change in thickness at each depth, $x_m(n)$, was obtained by the previous and proposed methods as shown in Figs. 6(f) and (g). Fig. 6(h) shows the actual change in thickness.

As shown in Fig. 6(f), the magnitudes of changes in thickness near the luminal surface estimated by the previous method became smaller than the actual change in thickness as described in Section II. However, as shown in Fig. 6(g), compounded changes in thickness, $\Delta \bar{h}(n; x)$, obtained by the proposed method were in good agreement with the actual changes in thickness shown in Fig. 6(h). Figs. 7(a) and 8(a) show the same actual change in thickness. Figs. 7(b) and 8(b) show waveforms of changes in thickness at points estimated by the previous and proposed methods, respectively, and Figs. 7(c) and 8(c) show the distributions of changes in thickness at $t = t_{\max}$ overlaid on the echo magnitude in the first frame ($t = 0$). Errors in the estimated changes in thickness obtained by the proposed method were only $0.19 \pm 0.04\%$ (mean \pm standard deviation) as compared with $21.2 \pm 24.1\%$ obtained by the previous method.

As shown in Fig. 8(c), changes in thickness estimated by the previous method around the lumen-intima interface were reduced as described in Section III. Such an artificial spatial variation of the changes in thickness estimated by the previous method was suppressed as shown in Fig. 7(c), and the change in thickness estimated at each depth is in good agreement with the change in intima-media thickness, which is defined as the true deformation using the proposed method.

C. Required Thickness of an Assigned Layer

In this section, errors in changes in thickness estimated with different thicknesses, $M_L \cdot \Delta x$, of an assigned layer were investigated to determine the required layer thickness. As shown in Fig. 4, the typical thickness of the intima-media complex of a carotid artery of a healthy subject without intimal thickening is about 0.5 mm. There-

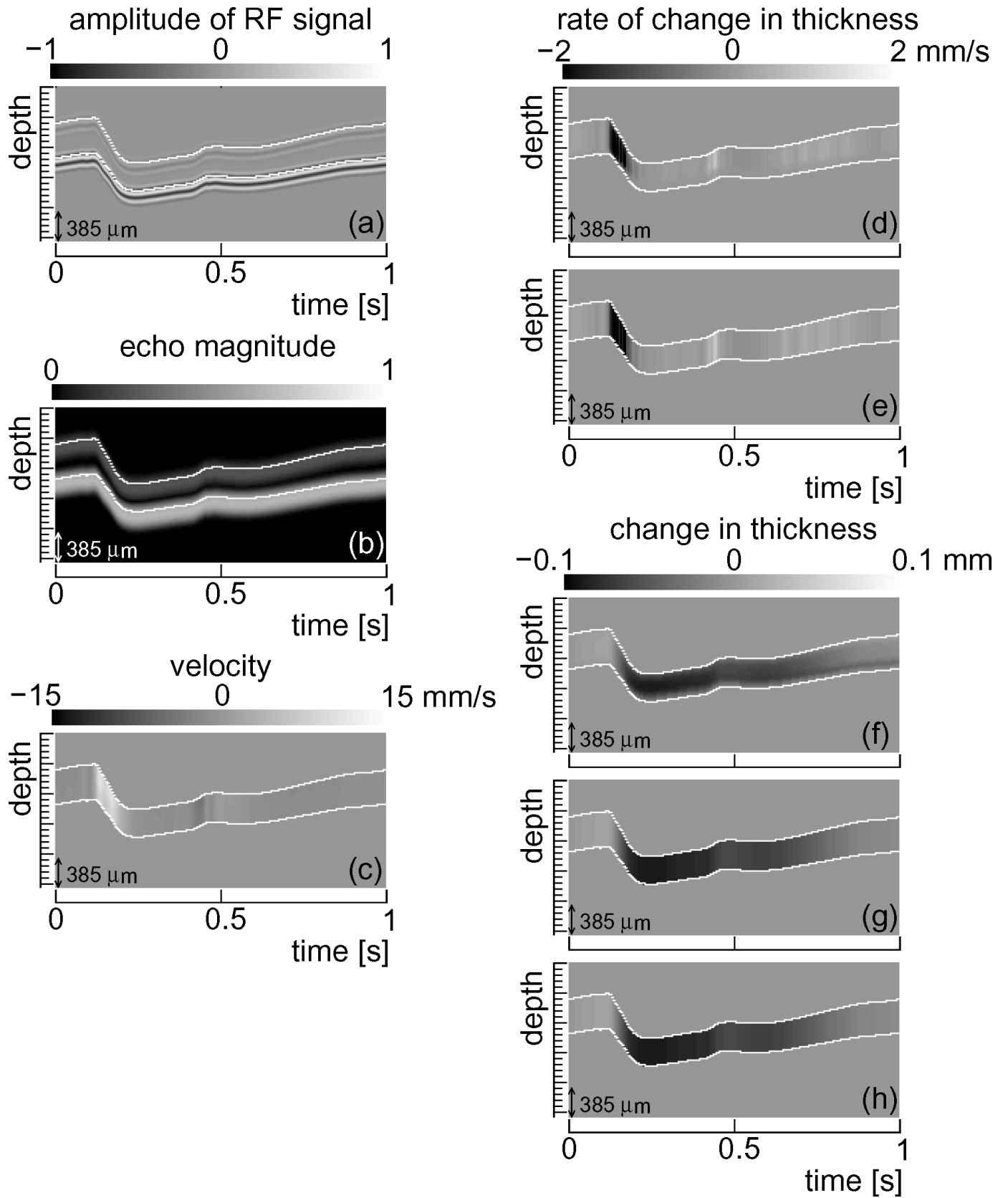


Fig. 6. Results of simulation experiments. (a) Simulated RF echo. (b) Magnitude of demodulated signal. (c) Velocity, $v_m(n)$. (d) and (e) Rates, $\Delta h'_m(n)$, of change in thickness obtained by the previous and proposed methods, respectively. (f) and (g) Changes in thickness, $\Delta h_m(n)$, obtained by the previous and proposed methods, respectively. (h) Actual change in thickness.

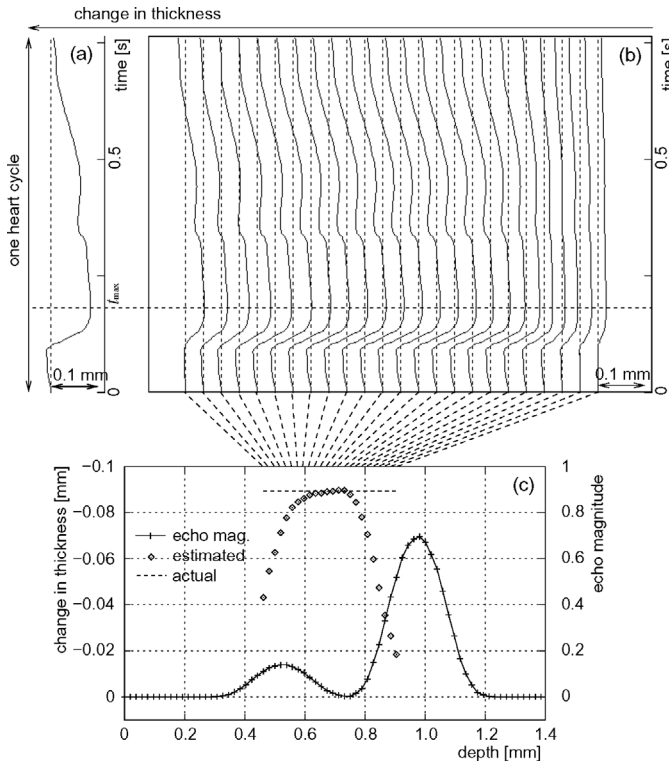


Fig. 7. Results of simulation experiments obtained by the previous phased-tracking method. (a) Waveform of the actual change in thickness. (b) Waveforms of changes in thickness estimated at various depths. (c) Magnitude of echo, actual change in thickness and estimated changes in thickness at t_{max} when the actual change in thickness is maximum.

fore, RF echoes were simulated for different cases of intima-media thicknesses of 0.4, 0.5, and 0.6 mm based on the principle described in Section IV-A.

In Fig. 9, errors in changes in thickness estimated by the proposed method are plotted as a function of the thickness, $M_L \cdot \Delta x$, of an assigned layer. As shown in Fig. 9, errors were reduced by increasing the layer thickness, $M_L \cdot \Delta x$. However, a larger layer thickness worsens the spatial resolution in the estimation of the change in thickness. Thus, it is desirable for the layer thickness, $M_L \cdot \Delta x$, to be as small as possible. As described in Section III, the duration of the ultrasonic pulse determines the lower limit of the layer thickness, $M_L \cdot \Delta x$, and this lower limit is found to be the width at -20 dB of the maximum magnitude of the quadrature demodulated signal. From these results, the layer thickness, $M_L \cdot \Delta x$, was determined to be $385 \mu\text{m}$ ($M_L = 20$).

V. IN VIVO EXPERIMENTS IN A HUMAN CAROTID ARTERY

Figs. 10(a) and (e) show the same electrocardiograms of a 30-year-old, healthy male. Fig. 10(b) shows the RF echo lines obtained in the region shown by the white, dashed line in Fig. 4(a). The frame rate and sampling frequency of simulated echoes were 286 Hz and 40 MHz, respectively.

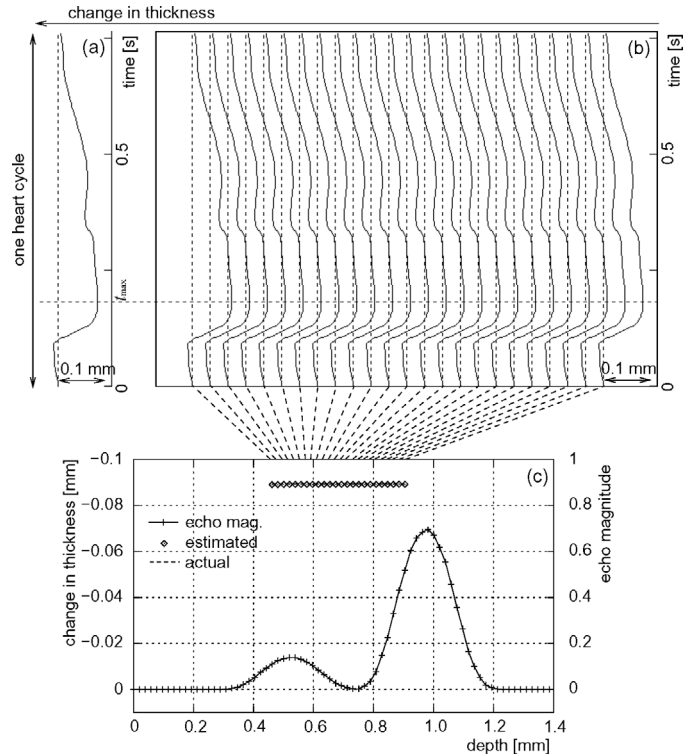


Fig. 8. Results of simulation experiments obtained by the proposed method. (a) Waveform of the actual change in thickness. (b) Waveforms of changes in thickness estimated at various depths. (c) Magnitude of echo, actual change in thickness and estimated changes in thickness at t_{max} when the actual change in thickness is maximum.

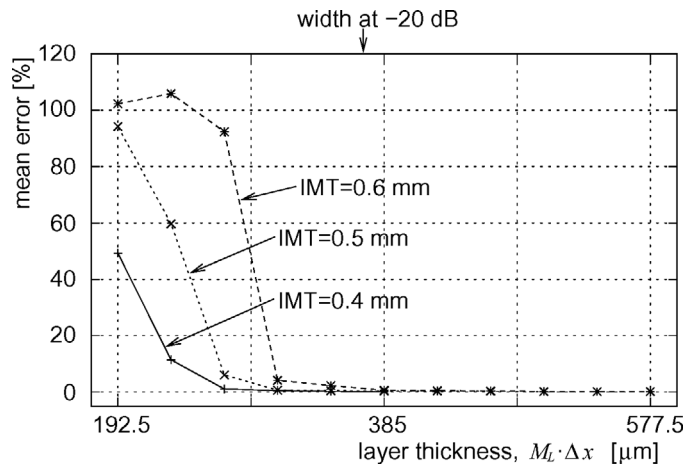


Fig. 9. Errors in changes in thickness estimated by the proposed method. Errors are plotted as a function of the layer thickness, $M_L \cdot \Delta x$, for different cases of IMTs.

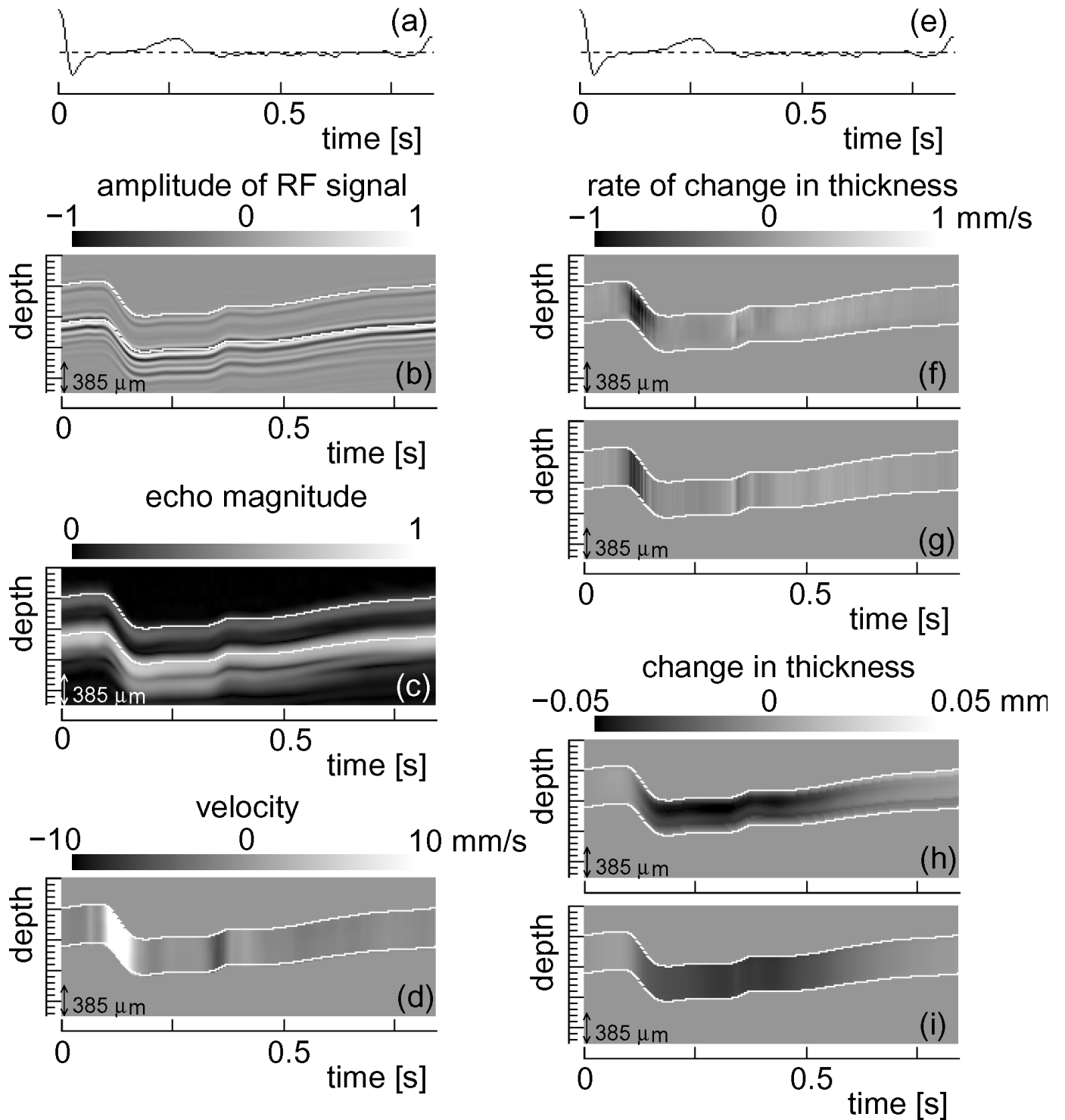


Fig. 10. Results of *in vivo* experiments in a carotid artery of a 30-year-old, healthy male. (a) and (e) Electrocardiograms. (b) Measured RF echo. (c) Magnitude of demodulated signal. (d) Velocity, $v_m(n)$. (f) and (g) Rates, $\Delta h'_m(n)$, of change in thickness obtained by the previous and proposed methods, respectively. (h) and (i) Changes in thickness, $\Delta h_m(n)$, estimated by the previous and proposed methods, respectively.

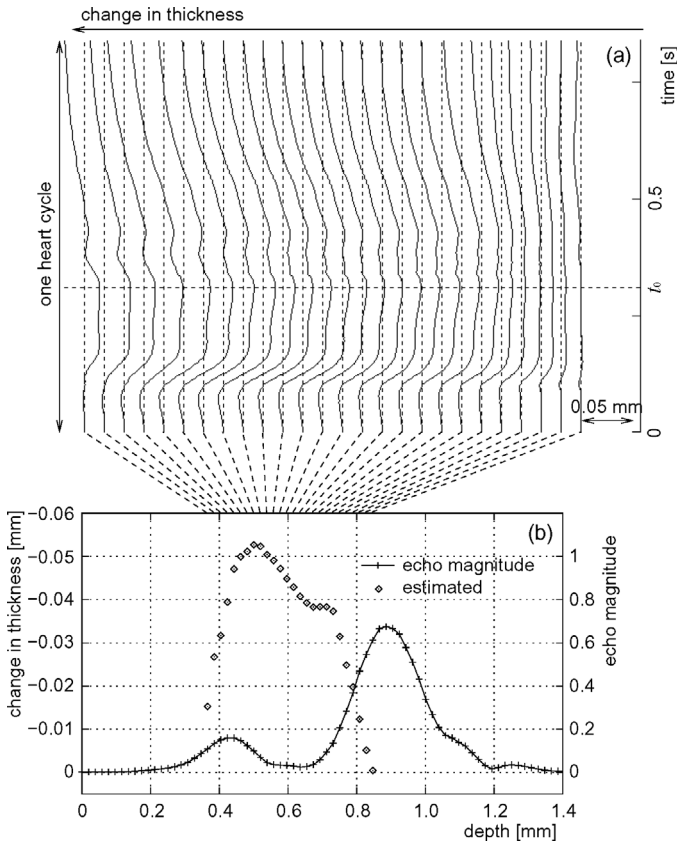


Fig. 11. Results of *in vivo* experiments obtained by the previous phased-tracking method. (a) Waveforms of changes in thickness estimated at various depths. (b) Magnitude of echo and estimated changes in thickness at $t = t_0$.

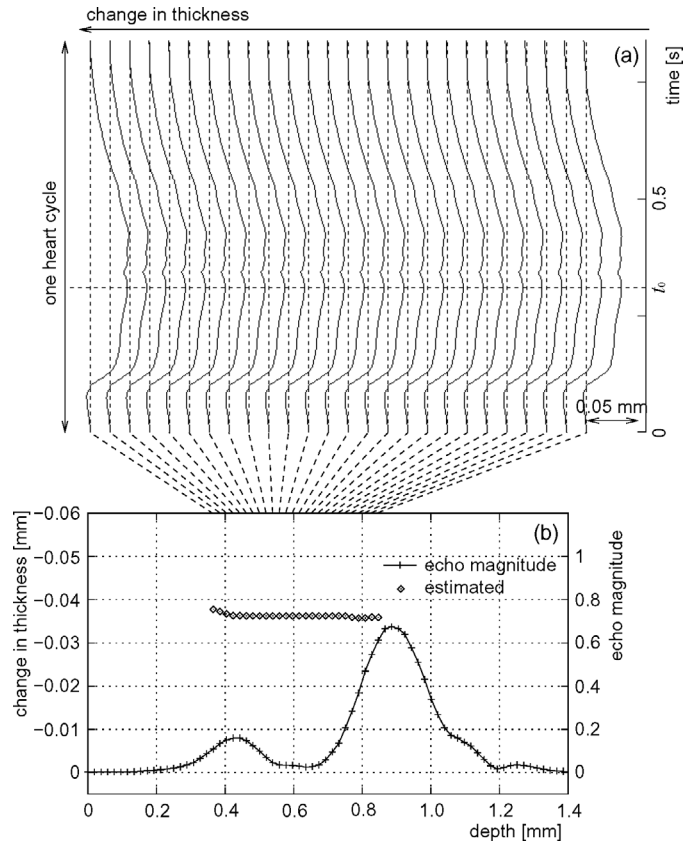


Fig. 12. Results of *in vivo* experiments obtained by the proposed method. (a) Waveforms of changes in thickness estimated at various depths. (b) Magnitude of echo and estimated changes in thickness at $t = t_0$.

Fig. 10(c) shows the M-mode image obtained from the measured RF echo lines shown in Fig. 10(b). By referring to the M-mode image shown in Fig. 10(c), the initial positions of the lumen-intima and media-adventitia boundaries were assigned manually at the first frame (time $t = 0$) by inspecting the M-mode image. With respect to multiple points between the assigned lumen-intima and media-adventitia boundaries, velocities, $v_m(n)$, at each point of time were estimated as shown in Fig. 10(d), and the instantaneous position of each point was tracked using the phased-tracking method. The estimated instantaneous positions of the lumen-intima and media-adventitia boundaries are shown by white lines in Fig. 10. Based on the instantaneous positions of the points assigned at $t = 0$ between the lumen-intima and media-adventitia boundaries, the rate of change in thickness at each depth, $x_m(n)$, was obtained by the previous and proposed methods as shown in Figs. 10(f) and (g), respectively. Along the instantaneous positions of each point at respective frames, the rate of change in thickness was integrated with respect to time, and the change in thickness, $\Delta h(n; x)$, at each depth was obtained by the previous and proposed methods as shown in Figs. 10(h) and (i), respectively.

Figs. 11(a) and 12(a) show waveforms of estimated changes in thickness at respective points, and Figs. 11(b)

and 12(b) show the distributions of changes in thickness at $t = t_0$ overlaid on the echo magnitude at the first frame. As shown in Fig. 11(b), the magnitude of changes in thickness near the luminal surface estimated by the previous method became smaller, as did those of the simulation experiments shown in Section IV. Changes in thickness between the lumen-intima and media-adventitia boundaries should be shown to be homogeneous because there are only two dominant echoes from these boundaries, and echoes from other scatterers in the wall hardly contribute to estimation of changes in thickness. As shown in Fig. 12(b), changes in thickness estimated by the proposed method have an almost homogeneous distribution, as also was the case in the simulation experiments.

As shown in Fig. 11(b), changes in thickness estimated by the previous method around the lumen-intima interface were reduced as described in Section III. As in the case of the simulation experiments, such an artificial spatial variation of the changes in thickness estimated by the previous method was suppressed using the proposed method as shown in Fig. 12(b). From these results, the proposed method was proved to properly show the deformation of the arterial wall, at least in the case in which there are two dominant echoes from the lumen-intima and media-adventitia interfaces.

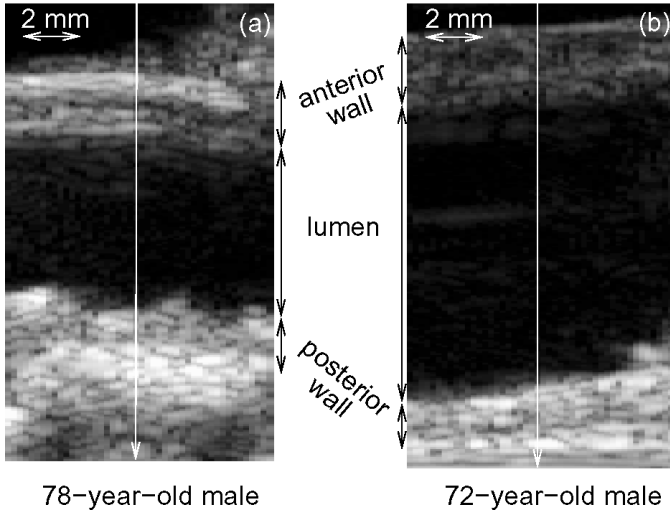


Fig. 13. B-mode images of femoral arteries excised from two patients with arteriosclerosis obliterans. (a) 78-year-old male. (b) 72-year-old male.

VI. IN VITRO EXPERIMENTS USING EXCISED DISEASED ARTERIES

Figs. 13(a) and (b) show B-mode images of femoral arteries excised from two patients, 78-year-old and 72-year-old males, with arteriosclerosis obliterans, respectively. After surgical extraction, arteries were immediately kept in cold storage and were measured within 5 days. These two arteries were placed in a water tank filled with 0.9% saline solution at the room temperature, and the change in internal pressure was applied by a flow pump. During the application of the change in internal pressure, RF lines were acquired along the ultrasonic beams as shown by white vertical arrows in Figs. 13(a) and (b). Then, as in the *in vivo* experiments, changes in thickness of the arterial walls were estimated by the previous and proposed methods as shown in Figs. 14–17. Figs. 14(a), 15(a), 16(a), and 17(a) show waveforms of internal pressure measured with a catheter (model 110-4, Camino Co., Ltd., San Diego, CA) located at the edge of the distal side of the artery. Figs. 14(b) and 16(b) show waveforms of changes in thickness of the 78-year-old and 72-year-old males, respectively, obtained by the previous method, and Figs. 15(b) and 17(b) show those obtained by the proposed method. Figs. 14(c), 15(c), 16(c), and 17(c) show the magnitudes of quadrature demodulated signals at time $t = 0$ and the changes in thickness at time $t = t_{\max}$ when the internal pressure was maximum. As in cases of the simulation and *in vivo* experiments, magnitudes of changes in thickness near the lumen-intima interfaces estimated by the previous method were small in comparison with those estimated by the proposed method. Such decreases in magnitudes of changes in thickness shown in Figs. 14(c) and 16(c) are considered to be artifacts as described in Section III, and such artifacts were reduced by the proposed method as shown in Figs. 15(c) and 17(c).

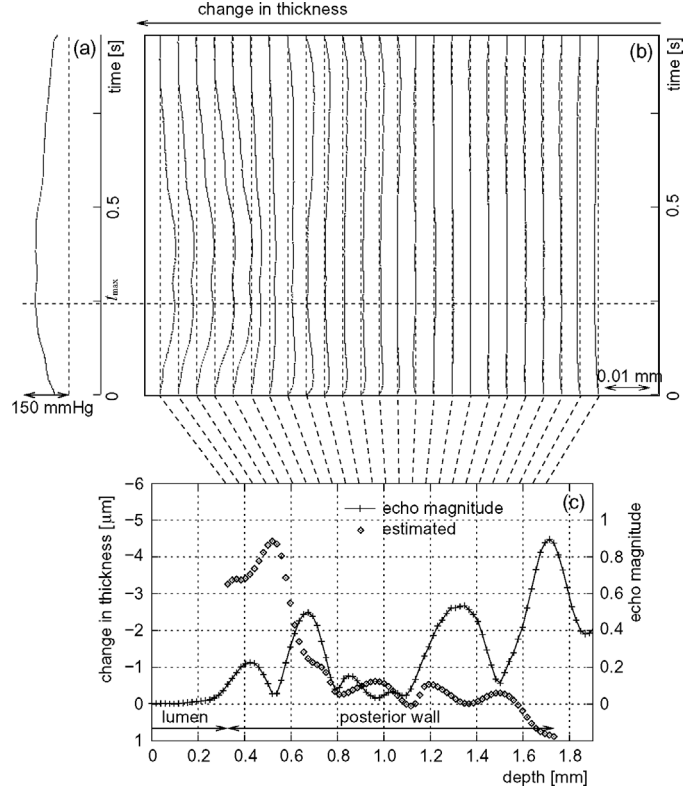


Fig. 14. Results of *in vitro* experiments obtained by the previous phased-tracking method (78-year-old male). (a) Internal pressure. (b) Waveforms of changes in thickness estimated at various depths. (c) Magnitude of echo and estimated changes in thickness at $t = t_{\max}$.

VII. DISCUSSION

In cases of diseased arteries shown in Fig. 13, there are spatial variations in estimated changes in thickness within arterial walls in comparison with an artery of a healthy subject. As shown in Figs. 15(c) and 17(c), the number of inflection points of spatial distribution of estimated changes in thickness were reduced in comparison with those of the previous method shown in Figs. 14(c) and 16(c) due to the deterioration of the spatial resolution caused by the enlargement of the thickness of an assigned layer. However, as described in Section IV-C, a layer thickness of at least the width at -20 dB of the maximum magnitude of the quadrature demodulated signal is required for reducing the artifact described in Section III. The elastic property of a diseased artery is heterogeneous, and the spatial variation in estimated changes in thickness within the arterial wall shown in Figs. 15(c) and 17(c) will be caused by such a heterogeneous distribution of elasticity. However, the effects of attenuation, diffraction, interference between echoes, and noise—which also influence the estimation of changes in thickness—were not considered in this study. The spatial variation in changes in thickness caused by a heterogeneous distribution of elasticity cannot be differentiated from that due to such effects. Therefore, further studies using phantoms with known mechanical properties such as those used in [11] are necessary for the validation

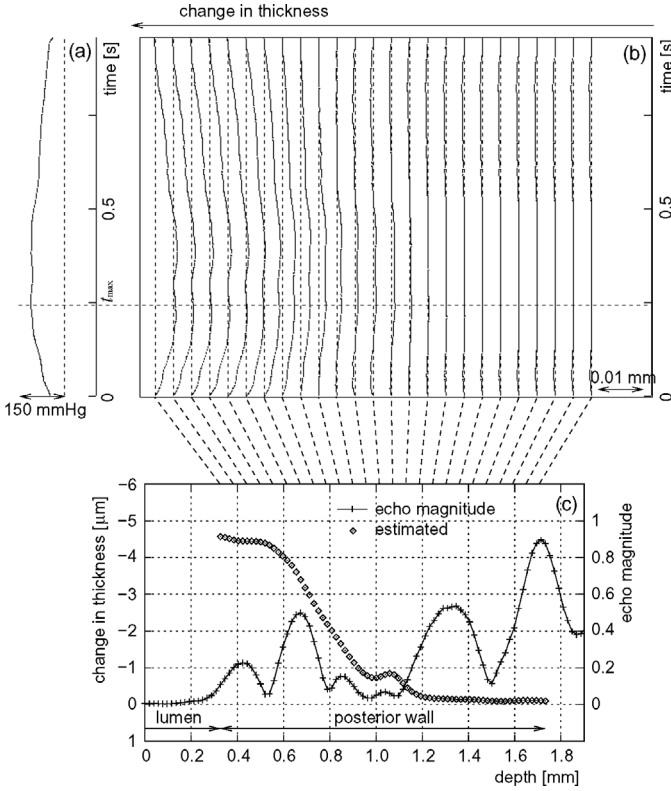


Fig. 15. Results of *in vitro* experiments obtained by the proposed method (78-year-old male). (a) Internal pressure. (b) Waveforms of changes in thickness estimated at various depths. (c) Magnitude of echo and estimated changes in thickness at $t = t_{\max}$.

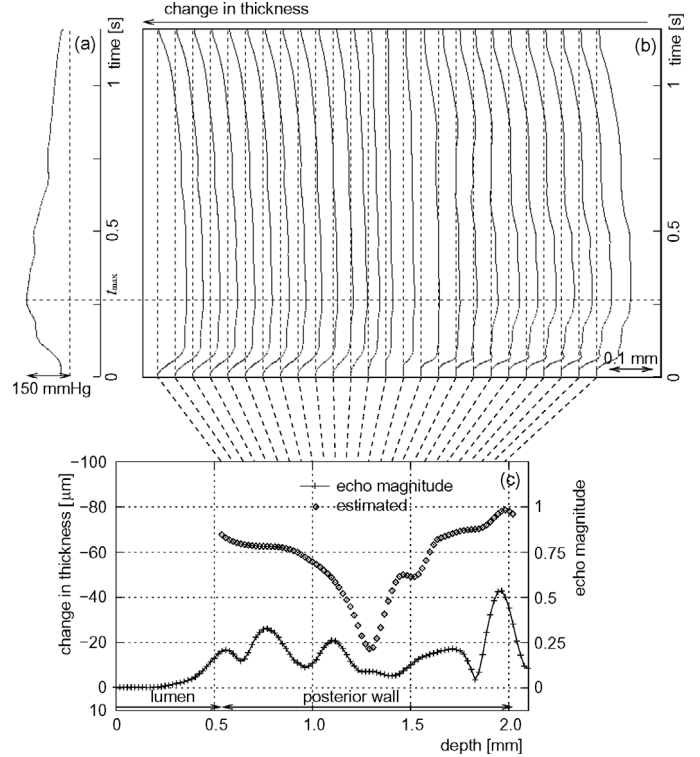


Fig. 17. Results of *in vitro* experiments obtained by the proposed method (72-year-old male). (a) Internal pressure. (b) Waveforms of changes in thickness estimated at various depths. (c) Magnitude of echo and estimated changes in thickness at $t = t_{\max}$.

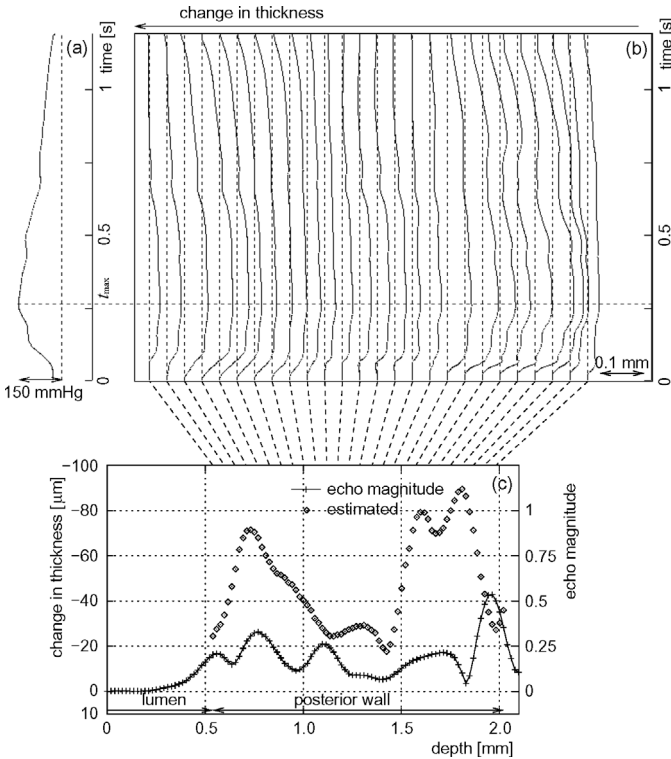


Fig. 16. Results of *in vitro* experiments obtained by the previous phased-tracking method (72-year-old male). (a) Internal pressure. (b) Waveforms of changes in thickness estimated at various depths. (c) Magnitude of echo and estimated changes in thickness at $t = t_{\max}$.

of the estimated changes in thickness within the wall like those shown in Figs. 15(c) and 17(c).

In addition, in this study, correlation estimators instead of rates of changes in thickness were compounded because the rate of the change in thickness contains no information on the signal-to-noise ratio of the echo signal used for estimating the change in thickness. By compounding the correlation estimators in (17), the contribution of a correlation estimator, which was obtained from the hypoechoic region (low signal-to-noise ratio), is suppressed. However, the effects of such compounding were not sufficiently investigated in this study, as it concentrated on the reduction of an artifact using the proposed method in cases of healthy subjects as described in Section III. Further investigations of the effects of compounding also are necessary.

In this study, measurements of changes in thickness were conducted for the posterior walls. As shown in Fig. 4(a), echoes from the lumen-intima interface of the anterior wall are often faint in comparison with those from the posterior wall. Such a phenomenon may be due to influences of echoes due to sidelobes of an ultrasonic beam, which are scattered by the soft tissue between the skin surface and the anterior wall.

VIII. CONCLUSIONS

In the present study, our previous method for measuring the change in thickness of the arterial wall caused by

the heartbeat was modified to reduce an artifact in a deformation image of the arterial wall.

In the case of a carotid artery of a healthy subject, there are only two dominant echoes from the lumen-intima and media-adventitia interfaces. In such a situation, only the change in the entire intima-media thickness can be estimated using ultrasound. However, changes in thickness estimated by the previous phased-tracking method show the artificial spatial variation. In this study, the phased-tracking method was modified to reduce this artifact. In simulation experiments, it was found that such artificial spatial variation was reduced by the proposed method, and changes in thickness estimated by the proposed method corresponded to that in the entire intima-media thickness. In addition, in *in vivo* experiments, a similar distribution of changes in thickness was obtained. A simple model corresponding to the measurement in carotid arteries of healthy subjects, in which there are only two dominant echoes from the lumen-intima and media-adventitia interfaces, was used in this study to elucidate the effect of modification. Therefore, more complex cases, in which there are more dominant echoes from the arterial wall, as in cases of atherosclerotic plaque, should be investigated in the future.

ACKNOWLEDGMENT

This work was supported by the Ministry of Education, Science, Sports and Culture, and is partially supported by the Mazda Foundation, the Nakatani Electronic Measuring Technology Association of Japan, and the Inamori Foundation.

REFERENCES

- [1] R. T. Lee, A. J. Grodzinsky, E. H. Frank, R. D. Kamm, and F. J. Schoen, "Structure-dependent dynamic mechanical behavior of fibrous caps from human atherosclerotic plaques," *Circulation*, vol. 83, pp. 1764–1770, 1991.
- [2] H. M. Loree, A. J. Grodzinsky, S. Y. Park, L. J. Gibson, and R. T. Lee, "Static circumferential tangential modulus of human atherosclerotic tissue," *J. Biomech.*, vol. 27, pp. 195–204, 1994.
- [3] M. Benthin, P. Dahl, R. Ruzicka, and K. Lindström, "Calculation of pulse-wave velocity using cross-correlation—effects of reflexes in the arterial tree," *Ultrasound Med. Biol.*, vol. 17, pp. 461–469, 1991.
- [4] H. Kanai, K. Kawabe, M. Takano, R. Murata, N. Chubachi, and Y. Koiwa, "New method for evaluating local pulse wave velocity by measuring vibrations on aortic wall," *Electron. Lett.*, vol. 30, pp. 534–536, 1993.
- [5] P. J. Brands, J. M. Willigers, L. A. F. Ledoux, R. S. Reneman, and A. P. G. Hoeks, "A noninvasive method to estimate pulse wave velocity in arteries locally by means of ultrasound," *Ultrasound Med. Biol.*, vol. 24, pp. 1325–1335, 1998.
- [6] A. Eriksson, E. Greiff, T. Loupas, M. Persson, and P. Pesque, "Arterial pulse wave velocity with tissue Doppler imaging," *Ultrasound Med. Biol.*, vol. 28, pp. 571–580, 2002.
- [7] J. M. Meinders, P. J. Brands, J. M. Willigers, L. Kornet, and A. P. G. Hoeks, "Assessment of the spatial homogeneity of artery dimension parameters with high frame rate 2-D B-mode," *Ultrasound Med. Biol.*, vol. 27, pp. 785–794, 2001.
- [8] A. P. G. Hoeks, C. J. Ruissen, P. Hick, and R. S. Reneman, "Transcutaneous detection of relative changes in artery diameter," *Ultrasound Med. Biol.*, vol. 11, pp. 51–59, 1985.
- [9] T. Länne, H. Stale, H. Bengtsson, D. Gustafsson, D. Bergqvist, B. Sonesson, H. Lecerof, and P. Dahl, "Noninvasive measurement of diameter changes in the distal abdominal aorta in man," *Ultrasound Med. Biol.*, vol. 18, pp. 451–457, 1992.
- [10] P. J. Brands, A. P. G. Hoeks, M. C. M. Rutten, and R. S. Reneman, "A noninvasive method to estimate arterial impedance by means of assessment of local diameter change and the local center-line blood flow velocity using ultrasound," *Ultrasound Med. Biol.*, vol. 22, pp. 895–905, 1996.
- [11] C. L. de Korte, E. I. Céspedes, A. F. W. van der Steen, and C. T. Lanée, "Intravascular elasticity imaging using ultrasound: Feasibility studies in phantoms," *Ultrasound Med. Biol.*, vol. 23, pp. 735–746, 1997.
- [12] E. I. Céspedes, C. L. de Korte, and A. F. W. van der Steen, "Intraluminal ultrasonic palpation: Assessment of local and cross-sectional tissue stiffness," *Ultrasound Med. Biol.*, vol. 26, pp. 385–396, 2000.
- [13] R. L. Maurice, É. Brusseau, G. Finet, and G. Cloutier, "On the potential of the Lagrangian speckle model estimator to characterize atherosclerotic plaques in endovascular elastography: *In vitro* experiments using an excised human carotid artery," *Ultrasound Med. Biol.*, vol. 31, pp. 85–91, 2005.
- [14] O. Bonnefous, "Blood flow and tissue motion with ultrasound for vascular applications," *Comptes Rendus de l'Académie des Sciences, Series IV, Physics*, vol. 2, pp. 1161–1178, 2001.
- [15] H. Ribbers, S. Holewijn, J. D. Blankensteijn, and C. L. de Korte, "Non-invasive two dimensional elastography of the carotid artery," in *Proc. IEEE Ultrason. Symp.*, 2005, pp. 1113–1116.
- [16] M. Cinthio, T. Jansson, Å. R. Ahlgren, H. W. Persson, and K. Lindström, "New non-invasive method for intima-media thickness and intima-media compression measurements," in *Proc. IEEE Ultrason. Symp.*, 2005, pp. 389–392.
- [17] H. Kanai, M. Sato, Y. Koiwa, and N. Chubachi, "Transcutaneous measurement and spectrum analysis of heart wall vibrations," *IEEE Trans. Ultrason., Ferroelect., Freq. Contr.*, vol. 43, pp. 791–810, 1996.
- [18] H. Kanai, H. Hasegawa, N. Chubachi, Y. Koiwa, and M. Tanaka, "Noninvasive evaluation of local myocardial thickening and its color-coded imaging," *IEEE Trans. Ultrason., Ferroelect., Freq. Contr.*, vol. 44, pp. 752–768, 1997.
- [19] H. Hasegawa, H. Kanai, Y. Koiwa, and N. Chubachi, "Noninvasive evaluation of Poisson's ratio of arterial wall using ultrasound," *Electron. Lett.*, vol. 33, pp. 340–342, 1997.
- [20] H. Kanai, Y. Koiwa, and J. Zhang, "Real-time measurements of local myocardium motion and arterial wall thickening," *IEEE Trans. Ultrason., Ferroelect., Freq. Contr.*, vol. 46, pp. 1229–1241, 1999.
- [21] H. Hasegawa, H. Kanai, and Y. Koiwa, "Modified phased tracking method for measurement of change in thickness of arterial wall," *Jpn. J. Appl. Phys.*, vol. 41, pp. 3563–3571, 2002.
- [22] H. Hasegawa, H. Kanai, N. Hoshimiya, and Y. Koiwa, "Evaluating the regional elastic modulus of a cylindrical shell with nonuniform wall thickness," *J. Med. Ultrason.*, vol. 31, pp. 81–90, 2004.
- [23] H. Kanai, H. Hasegawa, M. Ichiki, F. Tezuka, and Y. Koiwa, "Elasticity imaging of atheroma with transcutaneous ultrasound—Preliminary Study," *Circulation*, vol. 107, pp. 3018–3021, 2003.
- [24] J. Inagaki, H. Hasegawa, H. Kanai, M. Ichiki, and F. Tezuka, "Construction of reference data for tissue characterization of arterial wall based on elasticity images," *Jpn. J. Appl. Phys.*, vol. 44, pp. 4593–4597, 2005.
- [25] Q. Liang, I. Wendelhag, J. Wikstrand, and T. Gustavsson, "A multiscale dynamic programming procedure for boundary detection in ultrasonic artery images," *IEEE Trans. Med. Imag.*, vol. 19, pp. 127–142, 2000.
- [26] V. R. Newey and D. K. Nassiri, "Online artery diameter measurement in ultrasound images using artificial neural networks," *Ultrasound Med. Biol.*, vol. 28, pp. 209–216, 2002.
- [27] E. Falk, P. K. Shah, and V. Fuster, "Coronary plaque disruption," *Circulation*, vol. 92, pp. 657–671, 1995.
- [28] J. Golledge, R. M. Greenhalgh, and A. H. Davies, "The symptomatic carotid plaque," *Stroke*, vol. 31, pp. 774–781, 2000.
- [29] H. Hasegawa and H. Kanai, "Improving accuracy in estimation of artery-wall displacement by referring to center frequency of RF echo," *IEEE Trans. Ultrason., Ferroelect., Freq. Contr.*, vol. 53, pp. 52–63, 2006.

- [30] A. D. M. van Swijndregt, S. H. K. The, E. J. Gussenhoven, C. T. Lanée, H. Rijsterborgh, E. de Groot, A. F. W. van der Steen, N. Bom, and R. G. A. Ackerstaff, "An *in vitro* evaluation of the line pattern of the near and far walls of carotid arteries using B-mode ultrasound," *Ultrasound Med. Biol.*, vol. 22, pp. 1007–1015, 1996.
- [31] S. K. Jespersen, J. E. Wilhjelm, and H. Sillesen, "Multi-angle compound imaging," *Ultrason. Imag.*, vol. 20, pp. 81–102, 1998.



Hideyuki Hasegawa was born in Oyama, Japan, in 1973. He received the B.E. degree from Tohoku University, Sendai, Japan, in 1996. He received the Ph.D. degree from Tohoku University in 2001. He is presently a lecturer in the Graduate School of Engineering, Tohoku University.

His main research interest is medical ultrasound, especially diagnosis of atherosclerosis based on measurement of mechanical properties of the arterial wall.

Dr. Hasegawa is a member of the IEEE, the Acoustical Society of Japan, the Japan Society of Ultrasonics in Medicine, and the Institute of Electronics, Information and Communication Engineers.



Hiroshi Kanai (M'98) was born in Matsumoto, Japan, on November 29, 1958. He received a B.E. degree from Tohoku University, Sendai, Japan in 1981, and M.E. and the Ph.D. degrees, also from Tohoku University, in 1983 and in 1986, both in electrical engineering.

From 1986 to 1988 he was with the Education Center for Information Processing, Tohoku University, as a research associate. From 1990 to 1992 he was a lecturer in the Department of Electrical Engineering, Faculty of Engineering, Tohoku University. From 1992 to 2001 he was an associate professor in the Department of Electrical Engineering, Faculty of Engineering, Tohoku University. Since 2001 he has been a professor in the Department of Electronic Engineering, the Graduate School of Engineering, Tohoku University.

His present interests are in ultrasonic measurement and digital signal processing for diagnosis of heart diseases and arteriosclerosis.

Dr. Kanai is a member of the Acoustical Society of Japan, the Institute of Electronics Information and Communication Engineering of Japan, the Japan Society of Ultrasonics in Medicine, Japan Society of Medical Electronics and Biological Engineering, and the Japanese Circulation Society.